Graphite under compressive biaxial stress: Raman modes and Grüneisen parameters

Elena del Corro,[* 1] Alberto Otero de la Roza,[2,3] Mercedes Taravillo,[1] and Valentín G. Baonza[1]

[1] *MALTA-Consolider Team, Departamento de Química Física I, Facultad de Ciencias Químicas, Universidad Complutense de Madrid, Plaza de Ciencias 3, 28040-Madrid, SPAIN*

[2] *MALTA-Consolider Team, Departamento de Química Física y Analítica, Universidad de Oviedo, ES-33006, Oviedo, SPAIN*

[3] *School of Natural Sciences, University of California, Merced 5200 North Lake Road, Merced, California 95343, USA*

We study the behaviour of the most characteristic Raman contributions of highly oriented pyrolytic graphite at biaxial stresses up to 5 GPa. The use of moissanite anvils allows us to observe for the first time the evolution with stress of the disorder-induced D band along with all the overtones and combination bands in the Raman spectrum of graphite. Theoretical calculations at different pressures, performed within the Density Functional Theory, allow us to conclude that the D band process involves iTO phonons along the K-Γ direction. A complete set of Grüneisen parameters is reported; the analysis of the ratios of such parameters provides direct information on the intrinsic coupling and stress response for each phonon branch.

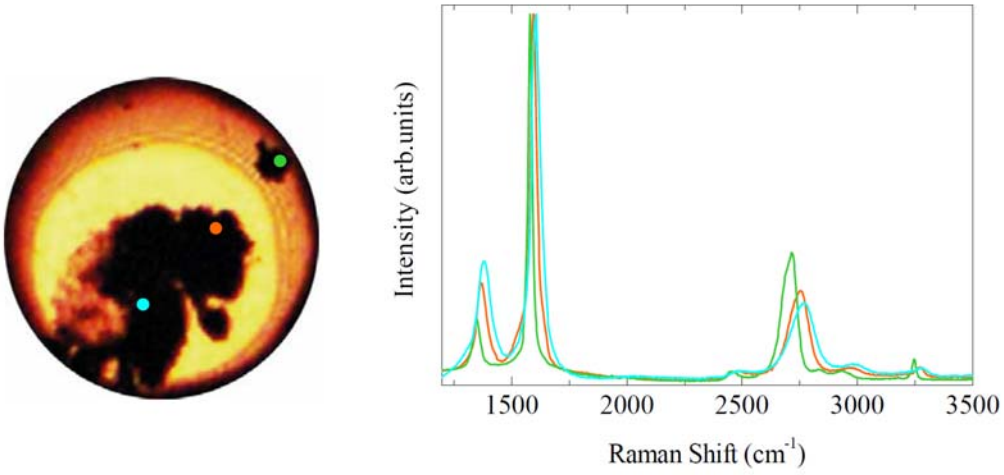

[*] Corresponding author. Fax: +34 91 394 4135. E-mail address: edelcorro@quim.ucm.es (Elena del Corro)

1. Introduction

Graphene and carbon nanotubes present remarkable mechanical properties that have motivated a large number of theoretical and experimental studies on carbon materials (CMs). Moreover, Raman spectroscopy is widely accepted as a convenient characterization technique [1] and suitable tool to analyse the strain state and its influence on the mechanical and electrical properties of these systems, including graphene [2]. Raman studies under stress have allowed the determination of the Grüneisen parameters for the G and 2D bands under tensile uniaxial and biaxial conditions [3,4]. However, despite graphite can be considered as the basic reference for many CMs, its behaviour under compressive stress is less known, and an analysis of the effect of the stress in the whole Raman spectrum of graphite is, in fact, lacking.

Both experiments and theoretical calculations on graphite under extreme stress or pressure conditions are currently focused on the phase transition reported to a new super-hard phase around 17 GPa [5-10], but detailed information about the behavior of graphite in the low to moderate compressive stress regime are scarce from the point of view of Raman spectroscopy.

The Raman spectrum of graphite was measured for the first time in 1970 [11] and its evolution with pressure was studied under both hydrostatic [12] and non-hydrostatic conditions [13]. However, in these previous works the only Raman band analyzed is the most intense contribution, known as the G band. This lack of information on the other Raman bands of graphite is due to the use of the diamond anvil cell, since the Raman bands of the diamond anvils overlap with most of the characteristic bands of graphite [14]. As we have recently demonstrated [14,15] the use of alternative gems allows a complete Raman characterization of CMs; in addition, interference with the pressure media [16-18], which has revealed as problematic, can be avoided by compressing the

specimen directly between the anvils, so subjecting the sample to biaxial compressive stress.

Several studies on carbon fibres have been carried out under tensile uniaxial stress, and the dependence of D, G and 2D bands up to 1% of strain has been reported [19]. However, significant tension-compression anisotropy has been found for graphite and graphene [20-22] and a complete study the compressive regime is demanded.

Another controversial issue concerns the origin of the disorder-induced bands, D and D'. Previous works [23-26] agree in that they are observed by the excitation of a phonon with $q \neq 0$ momentum (in the vicinity of K and Γ-points, respectively) due to the presence of defects in the sample. However, some discrepancies exist concerning the assignment of the phonon branch (LO [23-25] or iTO [26]) implicated in the appearance of the D band. It looks that the origin of the D' band is less controversial, as all previous works associate this band to the maximum in the LO phonon near the Γ-point. As we shall show below, combination of theoretical calculations of the phonon dispersion curves of graphite/graphene under pressure and Raman measurements under biaxial stress allow us to unambiguously associate the D band to the iTO phonon branch.

From the stress dependence of the Raman frequencies we obtain information about the Grüneisen parameters, which, under biaxial stress, are defined as [3]:

$$\gamma^i = \left(d\omega_i / d\varepsilon\right) \Big/ 2\,\omega_i^0 \qquad (1)$$

where ω_i and ω_i^0 are the frequencies of the i^{th} Raman band under stress and at ambient conditions, respectively, and ε is the biaxial strain. Under moderate stresses, the quantity $(d\omega_i/d\varepsilon)$ can be reasonably approximated by $(\omega_i - \omega_i^0)/\varepsilon$.

It must be noted that the study of the Grüneisen parameters in graphene involves several drawbacks, leading to significant discrepancies in the parameters reported so far [3, 4, 27, 28]. Perhaps the most important reasons for such discrepancies are the doping

phenomena related to the substrate and the definition of the stress conditions. Both drawbacks are minimized in our experiments since biaxial conditions are unaffected by variations in the Poisson ratio and no substrate or surrounding media are necessary. Graphite under moderate compressive biaxial stresses is expected to behave as unsupported graphene, free from doping effects, as confirmed in recent studies of graphene under pressure using a diamond anvil cell [27, 29]. In addition, the use of the moissanite anvil cell (MAC) allows to study the stress dependence of all the Raman features in graphite, even those bands with low intensity, such as the D' band and its overtone. Thus, we provide reliable values of the Grüneisen parameters for the most prominent Raman bands of graphite, some of them not measured before, remarkable results due to their implications in graphene and other CMs.

2. Experimental

Our experimental set up is based on a MAC coupled to a micro-Raman spectrometer described in detail elsewhere [30]. This device is equipped with a Spectra-Physics solid state laser operating at 532.0 nm, a 10x Mitutoyo long working distance objective coupled to a 10x Navitar zoom system and focused on to the slit of an ISA HR460 monochromator with a grating of 600 grooves mm^{-1} and a liquid nitrogen-cooled CCD detector (ISA CCD3000, 1024 x 256 pixels). These specifications along with a calibration of the system with a standard neon discharge lamp provide a spectral resolution of the reported spectra better than 4 cm^{-1}.

The samples are directly placed between the anvils without a gasket and pressure transmitting media. With this configuration, the stress profile on the sample varies depending on the considered region [14,15], as can be observed in Figure 1, where we show three photographs of the sample at different steps of the experiment. In the first

stage of the experiment (Figure 1a), the loaded stress is the highest, as revealed by the interference rings, which indicate the area where the anvils are in closest contact; in this case most of the sample is subjected to stress. As the cell is unloaded, the interference rings become smaller (Figure 1b), and we can find regions of the sample compressed as well as regions close to ambient conditions. Once the stress is completely released, the interference rings are not observed anymore (Figure 1c), and the whole sample is unstressed.

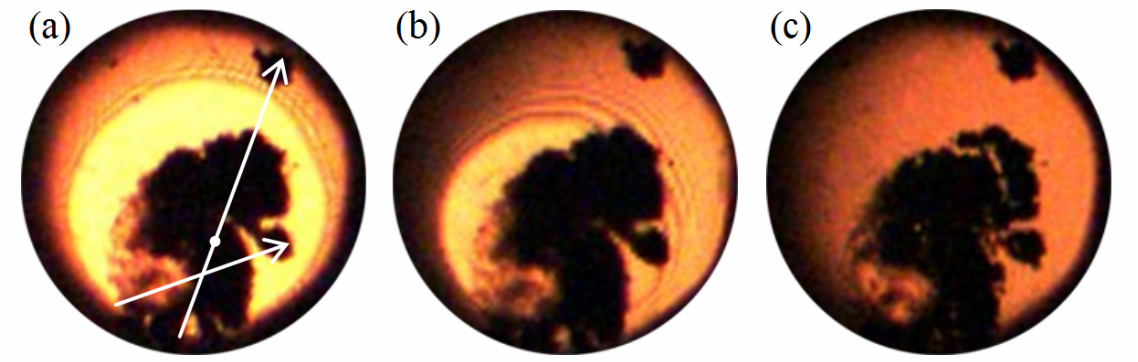

Figure 1. Photographs of the graphite sample directly compressed between the anvils, at three different stages of the experiment. The white spot and lines indicate the regions where the Raman spectra were registered.

Raman spectra were recorded at the center of the sample with increasing stress and along selected radial paths (white lines in Figure 1a) at different stages while stress is released. In order to measure these Raman spectra at different locations of the sample, the MAC is mounted on a XYZ stage and the laser light is directed to the sample by using a tiny focussing lens, providing excitation spots smaller than 20 μm.

As described in detail in ref. [14], the Raman spectra recorded in such fashion present contributions from both the sample and the front anvil. As already stared, the use of moissanite for CMs experiments avoids the intense interference of diamond [14].

In any case, the contribution of the second order spectra of moissanite must be properly subtracted for spectral analysis.

The absence of pressure media precludes the use of conventional pressure markers that would cause bridging between the anvils; for this reason, an alternative method to estimate the effective stress acting on the sample is required. Previous studies reveal that the frequency of the G band of graphite up-shifts with the same pressure slope independently of the stress conditions, hydrostatic [12] or non-hydrostatic [13]. This allows us to use the frequency of the G band to estimate the effective stresses (called σ_z) given in Figure 2a.

3. Calculations

The evolution of the phonon frequencies in the Γ-K path were calculated using DFT and Density Functional Perturbation Theory (DFPT) [31] as implemented in the Quantum ESPRESSO program [32]. The ultrasoft pseudopotential for carbon was obtained from the library included in the USSP program, by Vanderbilt [33]. The calculation parameters are: 60 Ry plane-wave cutoff, 16x16x8 k-point sampling and cold smearing [34] with a broadening parameter of 0.03 Ry. The geometries were determined by minimizing the enthalpy under the examined hydrostatic pressures (0, 4 and 8 GPa) with a threshold of 0.1 GPa. In order to obtain good interlayer separations, the DFT-D semiempirical dispersion correction [35] was used. The phonon frequencies were calcualted on a 8x8x8 grid and Fourier-interpolated to a finer q-grid: 50x50x50, that was then used to generate the phonon frequencies on the path. The strong anisotropy of graphite allows us to compare calculations under hydrostatic conditions with biaxial experiments without including biased geometrical restrictions in the computational procedure.

4. Results

In Figure 2 we show the Raman spectra of compressed graphite recorded at different sample locations in the 1200-3500 cm^{-1} spectral range. In order to show the less intense contributions to the Raman spectrum, two spectral regions are enlarged in Figures 2b and 2c.

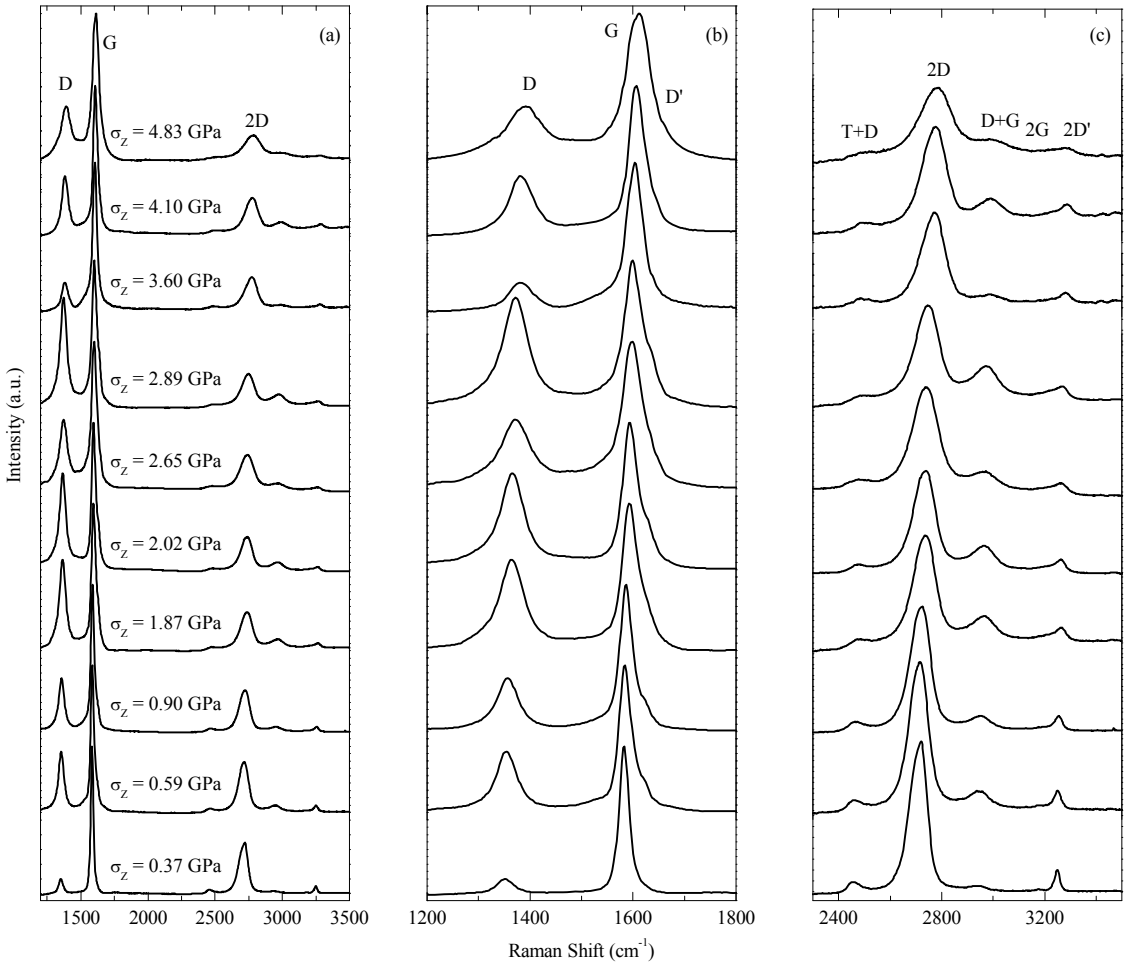

Figure 2. (a) Raman spectra of compressed graphite registered in different regions of the sample, along the white lines indicated in Figure 1. The spectra shown in (a) are split into two spectral regions: (b) fundamental bands from 1200 to 1800 cm^{-1} and (c) combination bands and overtones from 2300 to 3500 cm^{-1}.

After subtraction of the coincidental second order Raman background of moissanite [14], the bands of graphite can be clearly observed, including the D' band, which is less

intense, and those inaccessible using diamond anvils, such as the bands around 1350 (D band), 2935 (D+G band) and 2440 cm^{-1} (T+D band). A first observation reveals that the whole Raman spectra of graphite up-shifts and broadens with increasing stress. A similar correlation for the intensity of the defect-related bands is not observed [11, 36]. Thus, sample regions with higher concentration of defects present a Raman spectrum with a more intense D, D' (around 1622 cm^{-1}) and (D+G) features. Because the sample thicknesses studied in this work are inhomogeneous, the concentration of stress-induced defects varies among different sampled regions, finding higher defect concentration in thinner regions.

From the second derivative analysis of the spectra we obtain the frequency of all the Raman contributions, which are represented as a function of the frequency of the D band in Figure 3. The D band is chosen for this purpose because, in contrast to the G band, the frequency of the D band does not change with the crystal size in the basal plane of graphite, L_a, [37]. The analysis of the effects of L_a and defect concentration in the Raman spectrum present interesting findings which are out of scope of this work and will be published elsewhere [38]. As expected in a compressive regime, we see that all frequencies, even for those contributions appearing as shoulders in the spectrum (see Figures 3c and 3f), increase as the frequency of the D band, and so the biaxial stress, increases.

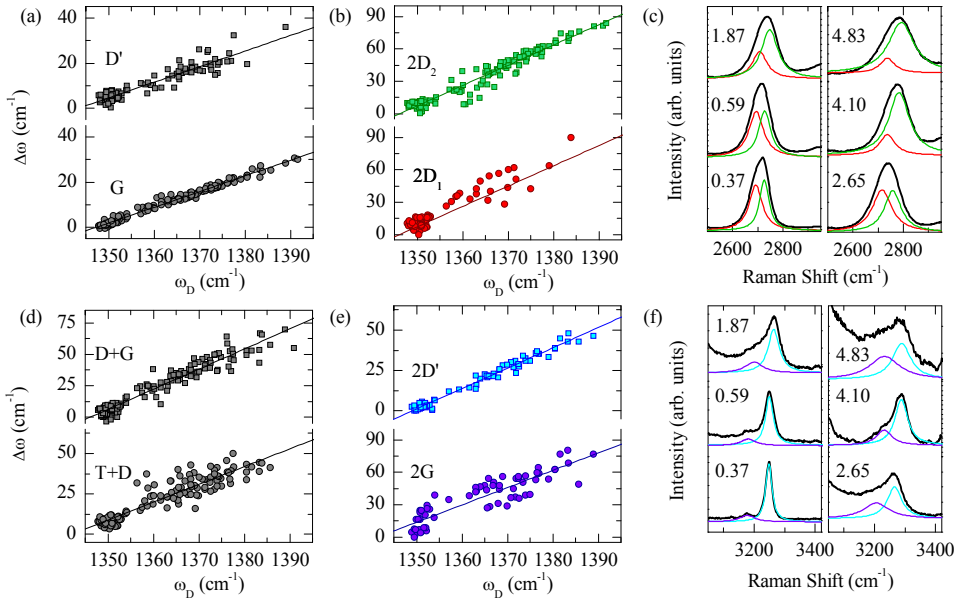

Figure 3. (a), (b), (d) and (e) Frequency shifts of the most intense Raman contributions of graphite as a function of the frequency of the D band. In order to calculate $\Delta\omega_i$, the reference ω_i^0 values listed in Table 1 were used. (c) and (f) enlarged Raman spectra of compressed graphite indicating the two contributions present in these spectral regions: (c) $2D_1$ and $2D_2$ bands and (f) 2G and 2D´ bands. The inserted numbers indicate the estimated effective stress σ_z (in GPa) on the sample.

The results for the D' band are particularly striking, because its stress dependence has not been reported so far. Although its frequency data show a larger scattering for being close in frequency to the intense G band, the second derivative analysis provides excellent results. The second derivative also allows distinguishing between the two contributions of the 2D band. Unfortunately, as we can observe in Figure 3b, spectral broadening at very high stresses sometimes precludes an accurate determination of the frequency of the $2D_1$. It is also striking the marked asymmetry of (T+D) band appearing around 2440 cm^{-1} that, along with its low intensity, causes the scattering in the frequencies observed for this contribution in Figure 3d, at least if it compared with the

variation in the (D+G) band; in any case, their stress dependencies are clearly characterized. In Figure 3f we can appreciate the intensity ratio between the 2G (around 3177 cm^{-1}) and 2D' (around 3247 cm^{-1}) bands and compare the linewidth of both contributions; these differences explain why the frequency of the 2D' band can be determined more accurately than that of the 2G band. Despite this fact, the shift of the 2G band can be measured even at high stress, when this band notably broadens. The stress slopes for all contributions are summarized in Table 1.

Table 1. Frequency at ambient conditions and with 532.0 nm excitation wavelength (ω_i^0), coefficients ($d\omega_i/d\omega_D$) and relation (γ_i/γ_G) for the most intense bands of the Raman spectrum of graphite.

Band	ω_i^0 (cm^{-1})	$d\omega_i/d\omega_D$	γ_i/γ_G
D	1350.2	1.000	1.7
G	1580.3	0.69 ± 0.01	1.0
D'	1622.2	0.69 ± 0.02	1.0
T+D	2442.2	1.01 ± 0.04	0.9
$2D_1$	2681.6	2.02 ± 0.08	1.7
$2D_2$	2722.2	1.88 ± 0.04	1.6
D+G	2934.9	1.60 ± 0.04	1.2
2G	3177.1	1.60 ± 0.10	1.2
2D'	3246.7	1.26 ± 0.02	0.9

We shall analyse first the assignment of the D band. As already mentioned, the phonon branch involved in the appearance of the D band is still unclear. Two scenarios are discussed in the literature: the LO [23-25] and the iTO [26] hypothesis. In view of the different stress coefficients of both D and D' bands (that of the D' band is 0.69 times that of the D band), we believe that these bands should arise from two different

phonon branches and, as the D' band is clearly associated to the LO phonon, the D band should be related to the iTO phonon along the Γ-K direction near the K-point.

In order to check this hypothesis we performed DFT calculations to estimate the evolution with stress of both LO and iTO phonon branches along the Γ-K direction. Results are shown in Figure 4 at three pressures: 0, 4 and 8 GPa. It is evident that the iTO phonon branch near the K-point present a larger energy shift with pressure than the LO phonon branch near the K-point. According to these results the pressure coefficient of the iTO phonon near the K-point is close to 6.0 cm^{-1}/GPa and the pressure coefficient of the LO phonon near the Γ-point is around 4.2 cm^{-1}/GPa; this corresponds to a coefficient ($d\omega_{LO}/d\omega_{iTO}$) of 0.7, in excellent agreement with our experiments ($d\omega_{D'}/d\omega_{D}$ = 0.69); whereas if we consider that the D band corresponds to the LO phonon near the K-point, we should obtain a coefficient ($d\omega_{D'}/d\omega_{D}$) of 1.3, in clear disagreement with our results.

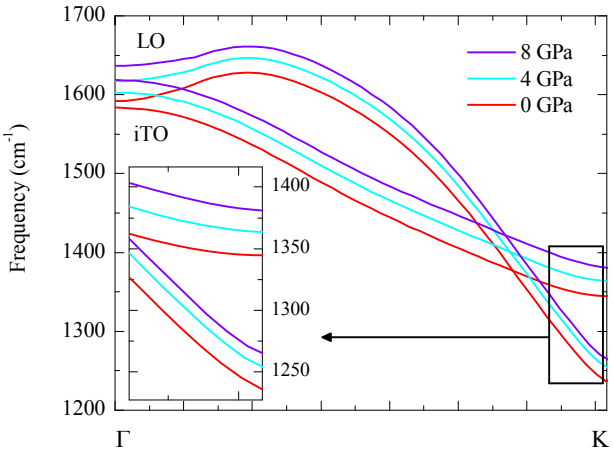

Figure 4. Evolution of the LO and iTO phonon branches calculated along the Γ-K direction under hydrostatic pressures at 0, 4 and 8 GPa.

Finally, the slopes ($d\omega_i/d\omega_D$) of the Table 1 can be used to determine the Grüneisen parameters, because the following relationship must hold between the Grüneisen parameter of each contribution and that of the G band:

$$\frac{\gamma^i}{\gamma^G} = \frac{\omega_G^0}{\omega_i^0} \frac{\left(d\omega_i / d\omega_D \right)}{\left(d\omega_G / d\omega_D \right)} \tag{2}$$

The results are reported in the last column of Table 1. In view of these data, we can conclude that the D band and its overtones ($2D_1$ and $2D_2$ bands) present a Grüneisen parameter larger than the G band, *i.e.* around 1.6 times γ^G; whereas for those vibrations in which the D band is not involved, such as D', 2G and 2D' bands, the Grüneisen parameters ratio is of the order of unity. This is in excellent agreement with previous results found in the literature for graphite, which are summarized in Table 2. In the case of graphene under tensile stress, the comparison with our results present some discrepancies probably due to the tension/compression anisotropy presented by both graphite and graphene [21-22].

Table 2. Relation between the Grüneisen parameter of each contribution and that of G band, γ^i/γ^G, for graphite and graphene.

	conditions	γ_D/γ_G	$\gamma_{D'}/\gamma_G$	γ_{2D}/γ_G	$\gamma_{2D'}/\gamma_G$
GRAPHITE	this work, biaxial compression	1.7	1.0	1.7	0.9
	hydrostatic compression[12,13,39,40,41]			1.57	0.96
GRAPHENE	uniaxial tension [3]			1.78	0.81
	biaxial tension/compression [42]	1.28		1.66	0.96
	biaxial tension [4]	1.40		1.44	0.92
	biaxial tension [43]			1.58	

The combination band (D+G) centred around 2935 cm^{-1} merits a detailed analysis, since it presents a relative Grüneisen parameter (1.2 times γ^G) larger than the G band but

not as large as the D band. To be more accurate, we can calculate the ratio (γ^{D+G} / γ^{G}) as a weighted average of our relative Grüneisen parameters of the D and G bands as:

$$\frac{\gamma^{D+G}}{\gamma^{G}} = \frac{\gamma^{D}}{\gamma^{G}}\frac{\omega_{D}^{0}}{\omega_{D+G}^{0}} + \frac{\gamma^{G}}{\gamma^{G}}\frac{\omega_{G}^{0}}{\omega_{D+G}^{0}} \quad (3)$$

With the data of Table 1 and this expression we obtain a calculated relative parameter of 1.3, in agreement with our experimental value.

For the band at 2442 cm^{-1} we assume the accepted assignment in the literature [44-47]. Previous experimental works, in which the Raman spectrum is studied with different excitation wavelengths [44] or at high temperature [45], agree in considering this band as the combination between the D and the 1083 cm^{-1} (only appreciated in defected samples and labelled as T band in ref. [45]) bands. This assignment does not differ with previous theoretical calculations that associate this band with the combination of the iTO and LA phonons [46] along the Γ-K direction [47]. Our Raman measurements as a function of stress also confirm this result, since the relative Grüneisen parameter obtained here is 0.9, in close agreement with the value of 1.0 calculated with the corresponding expression analogous to Eq. (3).

5. Conclusions

The stress dependence of the most relevant Raman features of graphite has been analyzed in detail under compressive biaxial stresses up to 5 GPa. To our knowledge, our experimental results for the stress dependence of the bands D, D´, T+D, D+G, 2G, 2D´ are the first reported so far.

In view of the different stress slopes presented by the resonant modes D and D' revealed by our experimental data and complemented with our theoretical calculations

of the optical phonon branches, the D and the D' bands have been assigned to the iTO and LO phonons, respectively.

The Grüneisen parameters of all the Raman bands relative to that of the G band were calculated from the variation with stress of the frequency of the Raman modes providing larger parameters for the D band and its overtones. Again, some of our results are reported for the first time here.

Overall, our experiments demonstrate that the comparison of the stress slopes (or equivalently, relative Grüneisen parameters) provides an appropriate framework to clarify controversial spectroscopic assignments in CMs and similar systems.

Acknowledgements

This research was supported by the Ministerio de Ciencia e Innovación under projects CTQ2009-14596-C02-01 and MALTA-Consolider Ingenio 2010 (CSD2007-00045). Funding was also provided by Comunidad de Madrid under program QUIMAPRES-S2009/PPQ-1551 and the grant No. UCM-BSCH-910481 from the Universidad Complutense de Madrid. E.d.C. is grateful to the spanish Ministerio de Educación for an FPU grant.

References

[1] Saito R, Hofmann M, Dresselhaus G, Jorio A, Dresselhaus MS. Raman Spectroscopy of graphene and carbon nanotubes, Adv Phys 2011;60:413-550.

[2] Frank O, Tsoukleri G, Riaz I, Papagelis K, Parthenios J, Ferrari AC, Geim AK, Novoselov KS, Galiotis C. Development of a universal stress sensor for graphene and carbon fibres. Nat Commun 2011;2: 2:255 | DOI: 10.1038/ncomms1247.

[3] Mohiuddin TMG, Lombardo A, Nair RR, Bonetti A, Savini G, Jalil R. Uniaxial strain in graphene by Raman spectroscopy: G peak splitting, Grüneisen parameters, and sample orientation. Phys Rev B 2009;79:205433.

[4] Zabel J, Nair RR, Ott A, Georgiou T, Geim AK, Novoselov KS, Casiraghi C. Raman spectroscopy of graphene and bilayer under biaxial Strain: bubbles and balloons. Nano Lett 2012;12:617-621.

[5] Mao WL, Mao H, Eng PJ, Trainor TP, Newville M, Kao C, Heinz DL, Shu J, Meng Y, Hemley RJ. Bonding Changes in Compressed Superhard Graphite. Science 2003;302:425-27.

[6] Li Q, Ma Y, Oganov AR, Wang H, Wang H, Xu Y, Cui T, Mao HK, Zou G. Superhard Monoclinic polymorph of Carbon. Phys Rev Lett 2009;102:175506.

[7] Umemoto K, Wentzcovitch RM, Saito S, Miyake T. Body-Centered Tetragonal C_4: a viable sp^3 carbon allotrope. Phys Rev Lett 2010;104:125504.

[8] Wang JT, Chen C, Kawazoe Y. Low-Temperature Phase Transformation from Graphite to sp^3 orthorhombic Carbon. Phys Rev Lett 2011;106:075501.

[9] Amsler A, Flores-Livas JA, Lehtorvaara L, Balima, F, Alireza Ghasemi S, Machon D, Pailhes S, Willand A, Caliste D, Botti S, San Miguel A, Goedecker S, Marques, MAL. Crystal Structure of Cold Compressed Graphite. Phys Rev Lett 2012,108:065501.

[10] Zhu Q, Oganov AR, Salvadó MA, Pertierra P, Lyakhov AO. Denser than diamond: Ab initio search for superdense carbon allotropes. Phys Rev B 2011;83:193410.

[11] Tuinstra F, Koenig JL. Raman spectrum of graphite. J Chem Phys 1970;53:1126-30.

[12] Hanfland M, Beister H, Syassen K. Graphite under pressure: equation of state and first-order Raman modes. Phys Rev B 1989;39:12598-603.

[13] Goncharov AF. Graphite at high pressures: amorphization at 44 GPa. High Press Res 1992;8:607-16.

[14] del Corro E, Taravillo M, González J, Baonza VG. Raman characterization of carbon materials under non-hydrostatic conditions. Carbon 2011;49:973-979.

[15] del Corro E, González J, Taravillo M, Flahaut E, Baonza VG. Raman spectra of double-wall carbon nanotubes under extreme uniaxial stress. Nano Lett 2008;8:2215-8.

[16] Puech P, Flahaut E, Sapelkin A, Hubel H, Dunstan D J, Landa G, Bacsa WS. Nanoscale pressure effects in individual double-wall carbon nanotubes Phys. Rev. B 2006, 73, 233408.

[17] Longhurst MJ, Quirke N. Pressure Dependence of the Radial Breathing Mode of Carbon Nanotubes: The Effect of Fluid Adsorption. Phys Rev Lett 2007;98,145503.

[18] Ghandour AJ, Dunstan DJ, Sapelkin A. Raman G-mode of single-wall Carbon Nanotube Bundles under Pressure. J. Raman Spectrosc. 2011;42,1611-1613.

[19] Galiotis G, Batchelder DN. Strain Dependences of the first- and second-order Raman spectra of carbon fibres, J Mat Sci Lett 1988;7:545-547.

[20] Gross TS, Nguyen K, Buck M, Timoshchuk N, Tsukrov II, Reznik B, Piat R, Böhlke T. Tension–compression anisotropy of in-plane elastic modulus for pyrolytic carbon. Carbon 2011;49:2145-47.

[21] del Corro E, Taravillo M, Baonza VG. Nonlinear strain effects in double-resonance Raman bands of graphite, graphene, and related materials. Phys Rev B 2012;85:033407.

[22] Tsoukleri G, Parthenios J, Papagelis K, Jalil R, Ferrari AC, Geim AK, Novoselov KS, C. Galiotis. Subjecting a Graphene Monolayer to Tension and Compression. Small 2009;5:2397-2402.

[23] Thomsen C, Reich S. Double resonant Raman scattering in graphite. Phys Rev Lett 2000;85:5214-17.

[24] Maultzsch J, Reich S, Thomsen C. Chirality-selective Raman scattering of the D mode in carbon nanotubes. Phys Rev B 2001;64:121407(R)-1-4.

[25] Kürti1 J, Zólyomi1 V, Grüneis A, Kuzmany H. Double resonant Raman phenomena enhanced by van Hove singularities in single-wall carbon nanotubes. Phys Rev B 2002;65:165433.

[26] Malard LM, Pimenta MA, Dresselhaus G, Dresselhaus MS. Raman spectroscopy in graphene. Phys Rep 2009;473:51-87.

[27] Proctor JE, Gregoryanz E, Novoselov KS, Lotya M, Coleman JN, Halsall MP. High-pressure Raman spectroscopy of graphene. Phys Rev B 2009;80:073408.

[28] Huang M, Yan H, Chen C, Song D, Heinz TF, Hone J. Phonon Softening and crystallographic orientation of strained graphene studied by Raman spectroscopy. Proc Natl Acad Sci USA 2009;106, 7304-7308.

[29] Nicolle J, Machon D, Poncharal P, Pierre-Louis O, San-Miguel A. Pressure-mediated doping in graphene. Nano Lett 2011;11:3564-68.

[30] Baonza VG, Taravillo M, Arencibia A, Cáceres M, Núñez J. Diamond as pressure sensor in high-pressure Raman spectroscopy using sapphire and other gem anvil cells. J Raman Spectrosc 2003;34:264-70.

[31] Baroni S, de Gironcoli S, Dal Corso A, Giannozzi P. Phonons and related crystal properties from density-functional perturbation theory. Rev Mod Phys 2001;73:515–562.

[32] Giannozzi P, et al. QUANTUM ESPRESSO: a modular and open-source software project for quantum simulations of materials. J Phys Condens Matter 2009;21:395502-1-19.

[33] Vanderbilt D. Soft self-consistent pseudopotentials in a generalized eigenvalue formalism. Phys Rev B 1990;41:7892-95.

[34] Marzari N, Vanderbilt D, de Vita A, Payne MC. Thermal Contraction and Disordering of the Al(110) Surface. Phys Rev Lett 1999;82:3296-99.

[35] Grimme S. Semiempirical GGA-type density functional constructed with a long-range dispersion correction. J Comp Chem 2006;27:1787-89.

[36] Nemanich RJ, Solin SA. First- and second-order Raman scattering from finite-size crystals of graphite, Phys Rev B 1979;20:392-401.

[37] Zerda TW, Xu W, Zerdab A, Zhaob Y, Von Dreeleb RB. High Pressure Raman and Neutron Scattering Study on Structure of Carbon Black Particles, Carbon 2000;38:355-61.

[38] del Corro E, Mechanical Response of graphite under extreme conditions. PhD Dissertation, Universidad Complutense de Madrid, June 2011.

[39] Sandler J, Shaffer M, Windle A, Halsall M, Montes-Moran M, Cooper C, Young R. Variations in the Raman Peak Shift as a Function of Hydrostatic Pressure for Various Carbon Nanostructures: A Simple Geometric Effect, Phys Rev B 2003;67:035417.

[40] Mounet N, Marzari N. First-Principles Determination of the Structural, Vibrational and Thermodynamic Properties of Diamond, Graphite and Derivatives, Phys Rev B 2005;71:205214.

[41] Goncharov A, Observation of amorphous phase of carbon at pressures above 23 GPa, JETP Lett 1990;51:418-421.

[42] Ding F, Ji H, Chen Y, Herklotz A, Dörr K, Mei Y, Rastelli A, Schmidt OG. Stretchable graphene: a close look at fundamental parameters through biaxial straining. Nano Lett 2010;10:3453-58.

[43] Metzger C, Remi S, Liu M, Kusminskiy SV, Castro Neto, AH, Swan AK, Goldberg BB, Biaxial Strain in Graphene Adhered to Shallow Depressions. Nano Lett 2010;10: 6-10.

[44] Kawashima Y, Katagiri G. Fundamentals, overtones, and combinations in the Raman spectrum of graphite. Phys Rev B 1995;52:10053-59.

[45] Tan P, Deng Y, Zhao Q. Temperature-dependent Raman spectra and anomalous Raman phenomenon of highly oriented pyrolytic graphite. Phys Rev B 1998;58:5435-39.

[46] Maultzsch, J, Reich, S, Thomsen, C. Double-resonant Raman scattering in graphite: Interference effects, selection rules, and phonon dispersion. Phys Rev B 2004;70:155403.

[47] Mafra, D, Samsonidze G, Malard L, Elias D, Brant J, Plentz F, Alves E, et al. Determination of LA and TO phonon dispersion relations of graphene near the Dirac point by double resonance Raman scattering. Phys Rev B 2007;76:233407.

Figure Captions

Figure 1. Photographs of the graphite sample directly compressed between the anvils, at three different stages of the experiment. The white spot and lines indicate the regions where the Raman spectra were registered.

Figure 2. (a) Raman spectra of compressed graphite registered in different regions of the sample, along the white lines indicated in Figure 1. The spectra shown in (a) are split into two spectral regions: (b) fundamental bands from 1200 to 1800 cm^{-1} and (c) combination bands and overtones from 2300 to 3500 cm^{-1}.

Figure 3. (a), (b), (d) and (e) Frequency shifts of the most intense Raman contributions of graphite as a function of the frequency of the D band. In order to calculate $\Delta\omega_i$, the reference ω_i^0 values listed in Table 1 were used. (c) and (f) enlarged Raman spectra of compressed graphite indicating the two contributions present in these spectral regions: (c) $2D_1$ and $2D_2$ bands and (f) 2G and 2D′ bands. The inserted numbers indicate the estimated effective stress σ_z (in GPa) on the sample.

Figure 4. Evolution of the LO and iTO phonon branches calculated along the Γ-K direction under hydrostatic pressures at 0, 4 and 8 GPa.

Tables

Table 1. Frequency at ambient conditions and with 532.0 nm excitation wavelength (ω_i^0), coefficients ($d\omega_i/d\omega_D$) and relation (γ_i/γ_G) for the most intense bands of the Raman spectrum of graphite.

Table 2. Relation between the Grüneisen parameter of each contribution and that of G band, γ^i/γ^G, for graphite and graphene.